Supplementary Materials

Neuronal Activity-Dependent Gene Dysregulation in C9orf72 i^{3}Neuronal Models of ALS/FTD Pathogenesis

Layla T. Ghaffari[1], Emily A. Welebob[1], Sarah E. B. Newton, Ashley V. Boehringer[1], Kelly L. Cyliax[1], Piera Pasinelli[1], Davide Trotti[1], Aaron R. Haeusler[1*]

Genotype	GroupID	Age of Onset	Sex	Onset	C9 Repeat Size	Insert / site	Lab Source
C9orf72	ALS/FTD	49	M	Lumbar	>44	Ngn1/2 + mCherry in CLYBL	Barmada lab
C9orf72	ALS/FTD	56	M	Cervical	>25	Ngn1/2 + mCherry in CLYBL	Barmada lab
Control	CTRL	NA	M	NA	normal	Ngn1/2 + iRFP in CLYBL	Barmada lab
Control	CTRL	NA	F	NA	normal	Ngn1/2 + mCherry in CLYBL	Barmada lab
C9orf72	ALS/FTD	NS	F	NA	NS	Ngn2 + mCherry in AAVS1	Ward lab
Control	CTRL	NA	M	NA	normal	Ngn2 in AAVS1	Ward lab

Supplemental Table 1. Source and demographic information for i^{3}Neuron lines used in this study, NA = not applicable, NS = not specified.

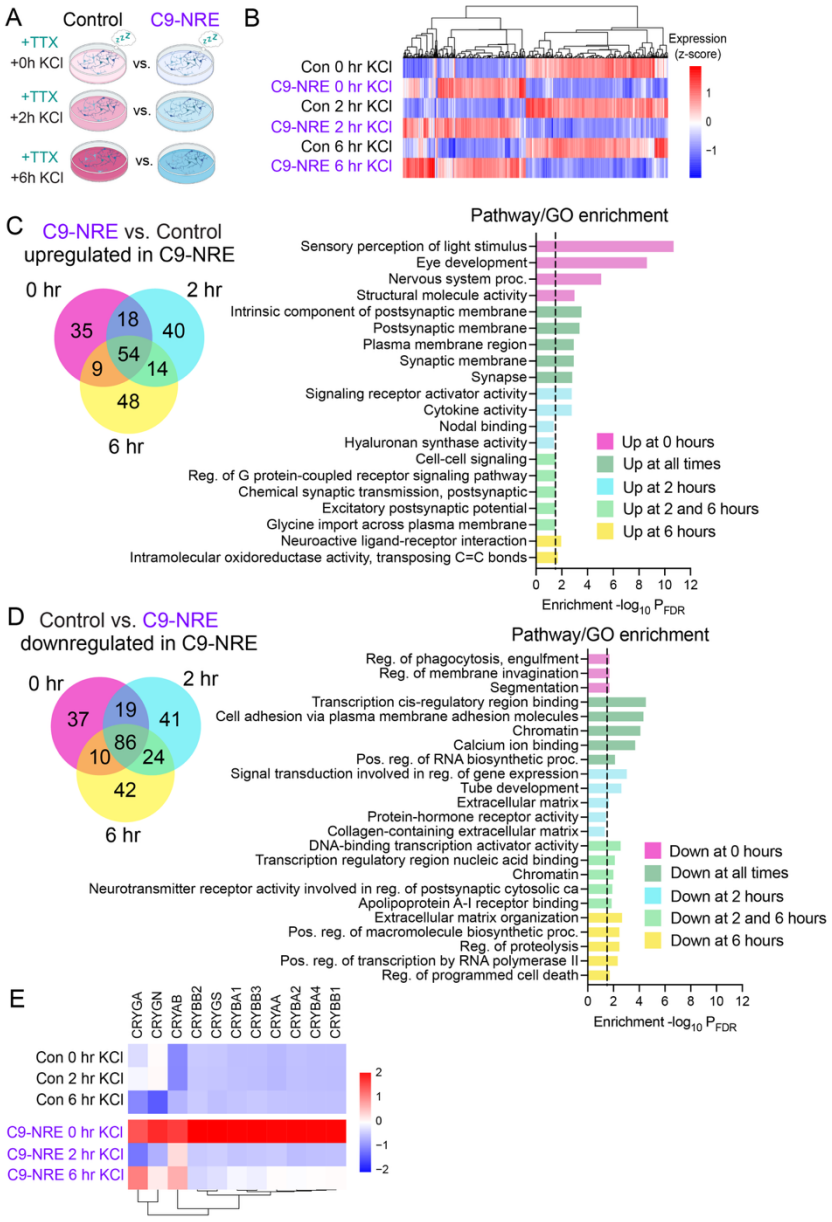

Supplemental Figure 1. Pairwise comparisons show C9-NRE i^{3}Neurons are enriched for receptor-signaling genes and are deficient in extracellular matrix-signaling pathways upon depolarization.

(A) Schema of origin of DEGs from DESeq2 used in Venn diagram comparisons. At each time point (0, 2, 6), Control i^{3}Neurons are compared to C9-NRE i^{3}Neurons. **(B)** Hierarchical clustering heatmap showing the gene expression (scaled by z-score) of pooled DEGs between listed comparisons in (A). (**C**) Venn diagram of DEGs shows the inherent transcriptomic differences between Control and C9-NRE i^{3}Neurons and how depolarization drives differential gene expression. Pathway Enrichment/GO are for transcripts upregulated in C9-NRE i^{3}Neurons. (**D**) same as in (B) but for down-regulated transcripts in C9-NRE i^{3}Neurons. (**E**) Hierarchical clustering heatmap showing widespread dysregulation of the crystallin family of genes in C9-NRE i^{3}Neurons.

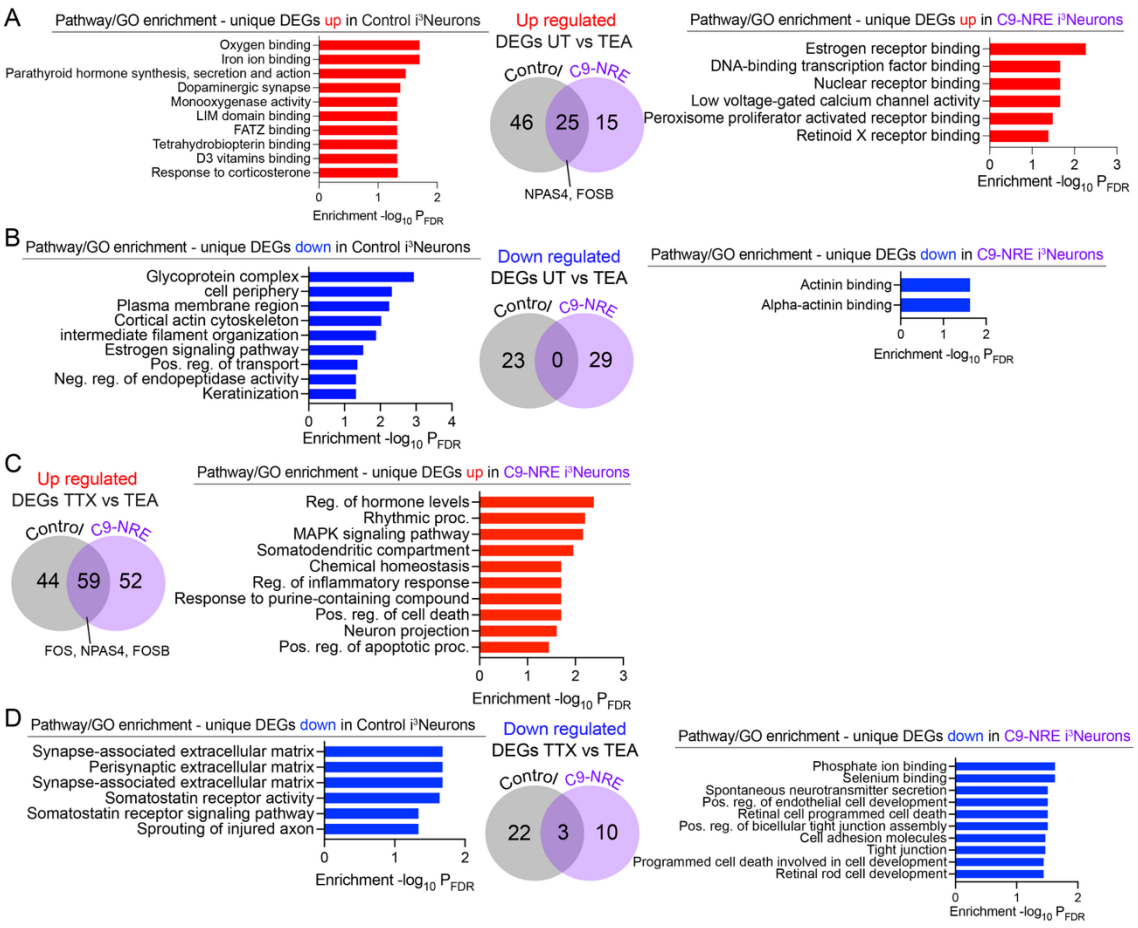

Supplemental Figure 2. Heatmaps of Clusters identified by maSigPro and peroxisomal gene dysregulation.

(A) DEG clusters were identified using maSigPro, using levels of neuronal activity as pseudo-time. **(B)** DEG clusters were identified using maSigPro, using levels of neuronal activity as pseudo-time with TEA stimulation, UT (untreated), and TTX silenced i^{3}Neurons. **(C)** A heatmap showing the dysregulation of peroxisome-associated genes in Control and C9-NRE i^{3}Neuron samples used in the KCl paradigm. **(D)** A heatmap showing the dysregulation of peroxisome-associated genes in Control and C9-NRE i^{3}Neuron samples used in the TEA paradigm.

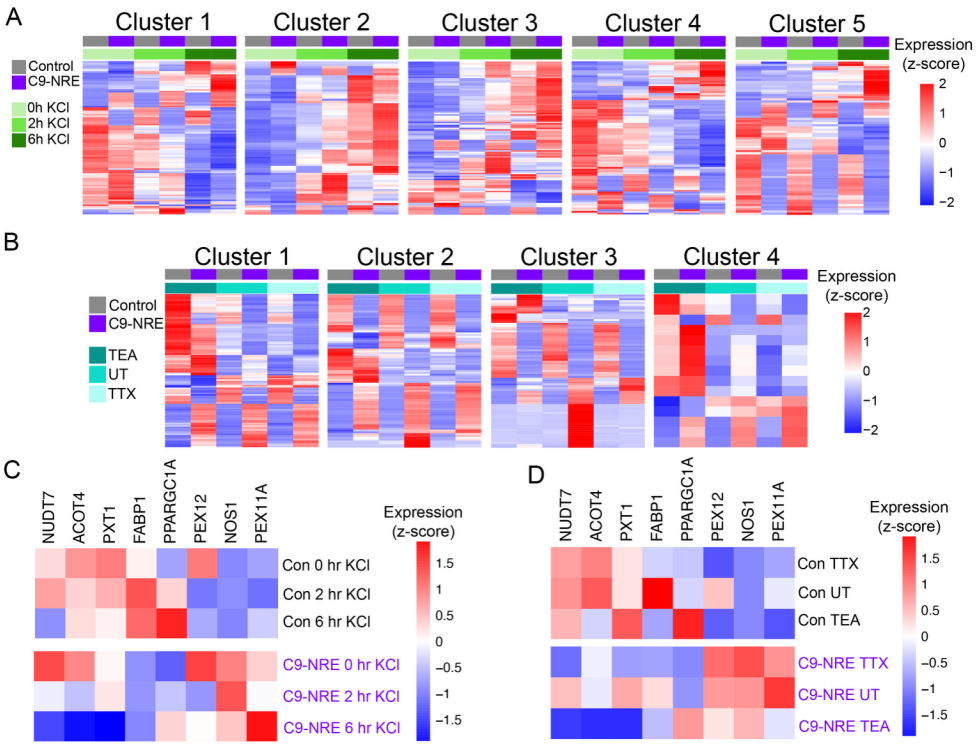

Supplemental Figure 3. Pairwise differential gene expression of TEA-stimulated and TTX-silenced i^{3}Neurons.

RNA Sequencing was performed on TTX-silenced and TEA-stimulated i^{3}Neurons, and differentially expressed genes (DEGs) were identified using DESeq2. Pairwise comparisons were performed between untreated (UT) and TEA stimulated, or TTX-silenced and TEA stimulated for both Control and C9-NRE i^{3}Neurons. The number of genes uniquely up-regulated or down-regulated in control or C9-NRE i^{3}Neurons are shown in the Venn diagrams. **(A)** Pathway and gene ontology (GO) analysis were performed on the uniquely up-regulated DEGs in either Control or C9-NRE i^{3}Neurons in UT vs. TEA **(B)** Same as in (A) but for down-regulated genes. **(C)** Pathway and gene ontology (GO) analysis were performed on the uniquely up-regulated DEGs in either Control or C9-NRE i^{3}Neurons in TTX vs. TEA. **(D)** Same as in (C) but for down-regulated genes.

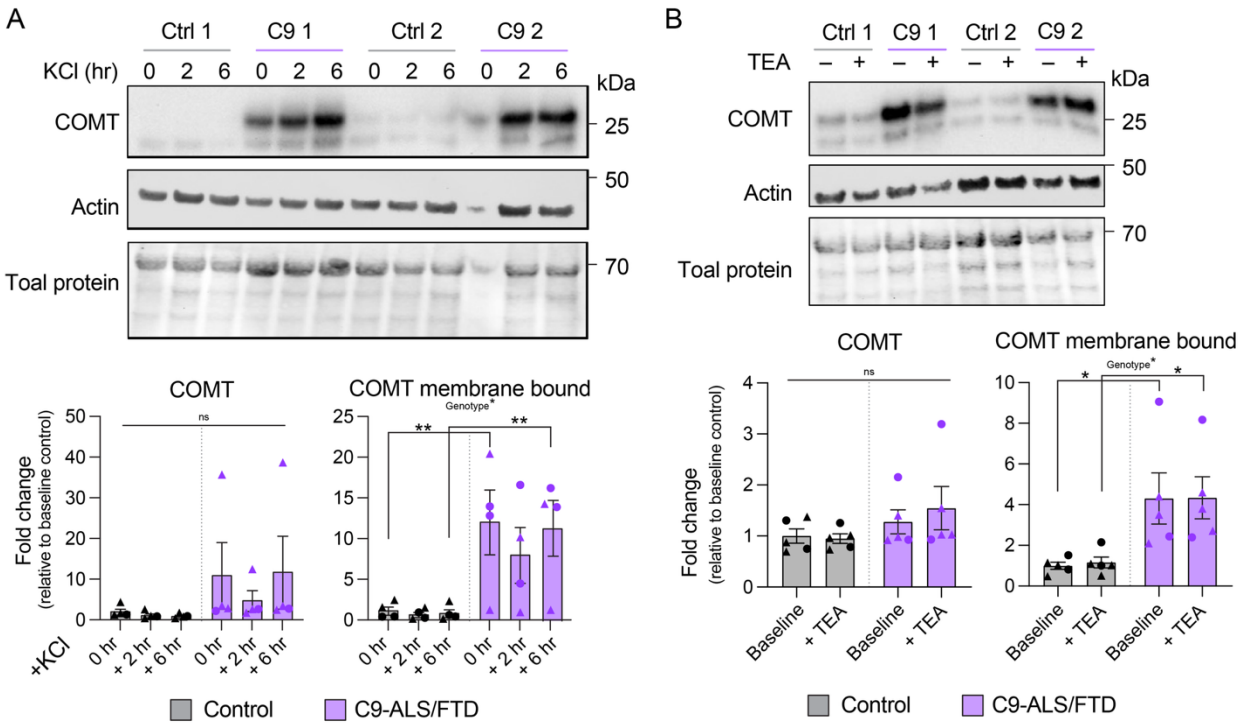

Supplemental Figure 4. Membrane-bound COMT is increased in C9 i^{3}Neurons.
(A) KCl paradigm. Representative immunoblots of whole-cell lysates from two independent lines per genotype (Ctrl 1–2; C9 1–2) collected at 0, 2, and 6 h after KCl. Blots were probed for COMT, actin, and total protein. Two COMT isoforms are visible: membrane-bound (~28 kDa, upper band) and soluble (~24 kDa, lower band). Molecular weight markers are indicated (25/50/70 kDa). No lanes were rearranged. Quantification (bottom) from *n* = 2 biological replicates and 2 independent differentiations. Intensities were expressed as fold change relative to the average control baseline (0 h) within each replicate. Symbols denote individual lines; color denotes genotype (gray = Control; purple = C9). Bars = mean ± SEM. Two-way mixed effects ANOVA (genotype × time) showed a main effect of genotype for membrane-bound COMT, with no effect for total COMT (ns). Sidak–Holm post hoc tests indicated C9 > Control at 0 h and 6 h ($p < 0.01$) for membrane-bound COMT. (**B**) TEA paradigm. Representative immunoblots from the same two lines per genotype under basal conditions (–) and after TEA (+). Membrane-bound and soluble COMT bands are indicated as in (A). Quantification (bottom) from *n* = 2 biological replicates with 2–3 independent differentiations. Data are plotted as fold change relative to the average basal control within each replicate; symbols and bars as in (A). Two-way mixed effects ANOVA (genotype × treatment) revealed a main effect of genotype for membrane-bound COMT, with total COMT not significant (ns). Asterisks indicate statistical significance of *$p < 0.05$; **$p < 0.01$; *ns = not significant.*

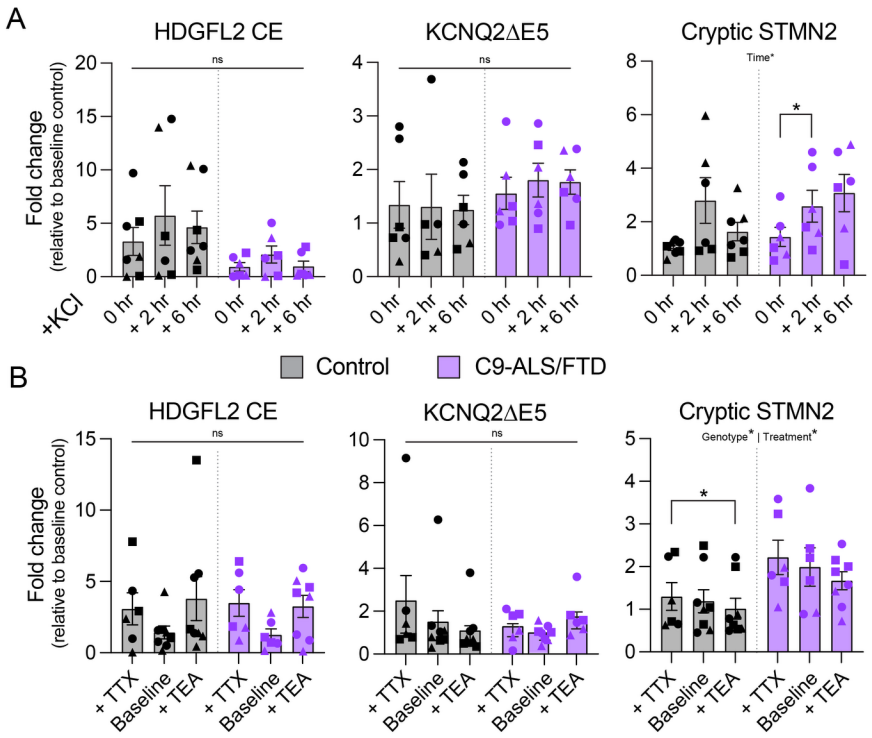

Supplemental Figure 5. Cryptic splicing is altered in C9 iPSC-derived neurons. (**A**) KCl stimulation paradigm. qPCR quantification of cryptic exon–containing transcripts (HDGFL2 CE, KCNQ2ΔE5, and cryptic STMN2) from control and C9-ALS/FTD iPSC-derived neurons following 0, 2, and 6 h of KCl stimulation. Data point color denotes cell line; shape denotes independent differentiation replicate. Each point represents the average of two technical qPCR replicates. ΔΔCT values were calculated by first normalizing raw CT values to RPLP0, then normalizing to the average ΔCT for control lines at 0 h. Bars show mean ± SEM. Two-way mixed effects ANOVA indicated a main effect of replicate for all three targets. Cryptic STMN2 additionally showed a main effect of stimulation time, with Tukey's post hoc test revealing a significant increase from 0 h to 2 h in C9 lines. (**B**) TEA and TTX paradigm. qPCR quantification of the same cryptic exon–containing transcripts under baseline (+TTX) and TEA treatment conditions. Data plotting and normalization as in (A), using baseline control values for ΔΔCT calculation. Two-way mixed effects ANOVA showed a main effect of genotype and treatment for STMN2 but not KCNQ2ΔE5 or HDGFL2. Tukey's multiple comparisons revealed a significant difference between TEA and TTX conditions in control lines. Asterisks indicate statistical significance of *$p < 0.05$; ns = not significant.